Journal Pre-proof

The effect of the chemical composition and structure of polymer films made from resorbable polyhydroxyalkanoates on blood cell response

Ekaterina I. Shishatskaya, Natalia G. Menzyanova, Anna A. Shumilova

PII: S0141-8130(19)35536-9

DOI: https://doi.org/10.1016/j.ijbiomac.2019.09.015

Reference: BIOMAC 13260

To appear in: *International Journal of Biological Macromolecules*

Received date: 17 July 2019

Revised date: 23 August 2019

Accepted date: 4 September 2019

Please cite this article as: E.I. Shishatskaya, N.G. Menzyanova and A.A. Shumilova, The effect of the chemical composition and structure of polymer films made from resorbable polyhydroxyalkanoates on blood cell response, *International Journal of Biological Macromolecules*(2019), https://doi.org/10.1016/j.ijbiomac.2019.09.015

THE EFFECT OF THE CHEMICAL COMPOSITION AND STRUCTURE OF POLYMER FILMS MADE FROM RESORBABLE POLYHYDROXYALKANOATES ON BLOOD CELL RESPONSE

Ekaterina I.Shishatskaya[1,2], Natalia G.Menzyanova[1], Anna A, Shumilova[1]

[1]*Siberian Federal University, 79 Svobodnyi Av., Krasnoyarsk 660041, Russia*

[2]*Institute of Biophysics SB RAS, Federal Research Center “Krasnoyarsk Science Center SB RAS”, 50/50 Akademgorodok, Krasnoyarsk 660036, Russia*

*Correspondence to: shumilova.ann@mail.ru

Abstract

Four PHA types were synthesized in the culture of *Cupriavidus eutrophus* B-10646 under special conditions, poly(3-hydroxybutyrate) [P(3HB)] and of copolymers, which contained 3HB monomers and 4-hydroxybutyrate (4HB), 3-hydroxyvalerate (3HV), or 3-hydroxyhexanoate (3HHx). All copolymers had the M_w of about 550-670 kDa, and the homopolymer P(3HB) had a significantly higher M_w – 920 kDa. P(3HB-co-4HB) and P(3HB-co-3HHx) had the lowest C_x (42 and 49%) while P(3HB-co-3HV) and P(3HB) exhibited higher C_x values (76%). Polymer films were prepared from different PHAs. Electron microscopy showed differences in the surface microstructure of the films. Films prepared from the P(3HB) were more hydrophobic and the arithmetic mean surface roughness of 71-75 nm, than the copolymer films, which were hydrophilic (57-60°) and had considerably higher roughness (158-177 nm). Blood parameters (hemoglobin and hemolysis) and response of the cells (erythrocytes, platelets, and monocytes) were studied in experiments with blood directly contacting the surface of the films of PHAs with different compositions. Cultivation of blood cells on polymer films did not cause any adverse effects on adhesion and morphology of all cell types. Results of studying blood cell response suggested that the films made from low-crystallinity copolymers containing 4-hydroxybutyrate and 3-hydroxyhexanoate were the best for contact with blood.

Keywords: degradable polyhydroxyalkanoates (PHAs), surface structure and properties, blood cell response.

1. INTRODUCTION

Development and investigation of new biocompatible materials for biomedical applications is one of the key tasks of the present time. Functional materials that can be used in contact with blood are needed to engineer artificial heart valves, small-diameter heart vessels, coronary stents, etc. These materials must not induce thromboses, activate the enzyme system of the blood embolisms, or adversely affect blood-forming elements[1].

Implanting stents in the arteries of patients with atherosclerosis is among the most frequently performed vascular interventions [2-4]. Intravascular implantation of the stent triggers a cascade of complex histopathologic processes – the organism's response to the invasion of a foreign body. The major limitation of stent implantation is development of restenosis – closure of the stented vessel as a biological response of the vessel wall to the foreign body invasion [5,6]. Decreasing of the risk of thrombosis remains the major issue of the post-operative period. Various approaches have been studied and used to enhance biocompatibility of stents, including coating of the stents with biocompatible materials (heparin, carbon and polymeric materials) and adding cytostatic drugs inhibiting hyperplasia of a neointima to stent coatings [7–11].

In addition to the commonly used polylactides and glycolides, promising biomaterials are natural resorbable microbial polymers polyhydroxyalkanoates (PHAs). Integrated biomedical studies of these polymers in cell culture and experiments with laboratory animals showed their high biocompatibility [12–17].

Biomaterials intended for long-term contact with blood must be subjected to particularly thorough scrutiny since hemocompatibility is the most important aspect of biological compatibility of biomaterials. However, the current literature presents just a few results of investigations of PHAs' blood compatible properties. There are fragmentary data on the absence of negative influence of PHB *in vitro* on hemolysis [18] and complement activation [19]. Research conducted at the Institute of Biophysics SB RAS and V.I. Shumakov Federal Research Center of Transplantology and Artificial Organs, Ministry of Health of the Russian Federation, proved that two high-crystallinity PHA types (poly-3-hydroxybutyrate and poly-3-hydroxybutyrate-co-3-hydroxyvalerate) contacting the blood did not cause adverse responses such as hemolysis, platelet aggregation, induction of enzyme systems of the blood [20]. Therefore, poly-3-hydroxybutyrate was subsequently used as a coating for the “Alex” nitinol vascular stents (Russia), in order to enhance their biocompatibility [21]. Experiments on laboratory animals showed the effectiveness of coating the stents with P(3HB) and the benefits of the addition of an antiproliferative drug for the alleviation of vessel wall reaction [22]. These results suggest that PHAs are promising materials for enhancing biocompatibility of blood-contacting implants. However, only the high-crystallinity P(3HB) and P(3HB-co-3HV) have been tested as blood-contacting materials while the mechanisms of interaction with blood cells of the more readily processable PHA copolymers, which have lower degrees of crystallinity and can be used to fabricate flexible and mechanically strong products, remain unknown.

The present study, for the first time, investigated responses of blood cells contacting with the surface of films fabricated from four PHA types with different chemical compositions, which differed considerably in their degrees of crystallinity and surface properties.

2. MATERIAL AND METHODS.

2.1. PHA synthesis

The strain used in this study was *Cupriavidus eutrophus* B-10646, registered in the Russian Collection of Industrial Microorganisms (RCIM) [23]. Chemolithoorganotrophic bacteria of the genus *Cupriavidus* (formerly known as *Ralstonia*) are regarded as very promising PHA producers, as these bacteria are capable of synthesizing different PHAs in very high yields (80-90% of cell dry weight) from various substrates. The mineral medium was used as a basic solution for growing cells: $Na_2HPO_4{\cdot}H_2O$ – 9.1; KH_2PO_4 – 1.5; $MgSO_4{\cdot}H_2O$ – 0.2; $FeC_6H_5O_7{\cdot}7H_2O$ – 0.025; $CO(NH_2)_2$ - 1.0 (g/L). Nitrogen was provided in the form of urea, and, thus, no pH adjustment was needed. The pH level of the culture medium was stabilized at 7.0±0.1. A solution of iron citrate (5 g/L), which was used as a source of iron, was added to reach a concentration of 5 ml/L. Hoagland's trace element solution was used: 3 ml of standard solution per 1 L of the medium. The standard solution contains H_3BO_3 – 0.288; $CoCl_2{\cdot}6H_2O$ – 0.030; $CuSO_4{\cdot}5H_2O$ – 0.08; $MnCl_2{\cdot}4H_2O$ – 0.008; $ZnSO_4{\cdot}7H_2O$ – 0.176; $NaMoO_4{\cdot}2H_2O$ – 0.050; $NiCl_2$ – 0.008 (g/L).

Homopolymer of 3-hydroxybutyric acid [P(3HB-)] was synthesized from a sole carbon source, glucose (China, purity: 98%). Synthesis of PHA copolymers [P(3HB-co-4HB), P(3HB-co-3HV)] or P(3HB-co-3HHx)] was achieved as follows: after 12-15 h of cultivation, nitrogen supply was discontinued, and the culture medium was supplemented with precursor substrates (ε-caprolactone, valeric acids or hydroxyhexanoic acids in the form of potassium salts) (Alfa Aesar, Germany).

To cultivate bacteria in shake flask culture, an Innova 44 constant temperature incubator shaker (New Brunswick Scientific, U.S.) was used. Inoculum was prepared by resuspending the museum culture maintained on agar medium. Museum culture was grown in 2.0 L glass flasks half-filled with saline liquid medium, with the initial concentration of glucose 15 g/L.

A two-stage process was used. In the first stage (20-25 h), cells were grown under nitrogen deficiency: the amount of nitrogen supplied in this stage was 60 mg/g cell biomass synthesized (i.e. 50% of the cells' physiological requirements – 120 mg/g). In the second stage (25-30 h), cells were cultured in nitrogen-free medium; the other parameters were the same as in the first stage. The temperature of the culture medium was 30±0.5°C and pH was 7.0±0.1.

2.2. Analysis of PHAs

Intracellular polymer content at different time points was determined by analyzing samples of dry cell biomass. Intracellular PHA content and composition of extracted polymer samples were analyzed using a GC-MS (6890/5975C, Agilent Technologies, U.S.). Both lyophilized cells and extracted polymer were subjected to methanolysis in the presence of sulfuric acid, and polymer was extracted and methyl esterified at 100°C for 3 h. Benzoic acid was used as an internal standard to determine total intracellular PHA.

Molecular weights and molecular weight distributions of PHA were examined using a gel permeation chromatograph (Agilent Technologies 1260 Infinity, U.S.) with a refractive index detector, using an Agilent PLgel Mixed-C column. Chloroform was the eluent. Calibration was made using polystyrene standards (Fluka, Switzerland, Germany). Molecular weights (weight average, Mw, and number average, Mn) and polydispersity (Đ = Mw/Mn) were determined.

Thermal analysis of PHA specimens was performed using a DSC-1 differential scanning calorimeter (METTLER TOLEDO, Switzerland). The specimens were heated at a rate of 5 °C/min to 200 °C, then cooled to -20 °C, held for 20 minutes and re-heated to 320 °C. Crystallization temperature (T_c), melting point (T_{melt}) and thermal degradation temperature (T_{degr}) were determined from peaks in thermograms using the “StarE” software.

X-ray structure analysis of PHAs was performed employing a D8ADVANCE X-ray powder diffractometer equipped with a VANTEC fast linear detector, using CuKa radiation (‘Bruker, AXS’, Germany). The degree of crystallinity was calculated as a ratio of the total area of crystalline peaks to the total area of the radiograph (the crystalline + amorphous components).

2.3. Extraction and purification of PHAs

PHAs are extractable from bacterial biomass due to their ability to dissolve in organic solvents and to be then precipitated by alcohols. The PHAs were extracted from bacterial biomass with chloroform and precipitated with ethanol. The extraction of PHAs from biomass was conducted in several stages. In the first stage, to partially destroy the cell wall and attain a fuller extraction of lipids, the bacterial biomass was centrifuged (for 15 min at 6000 rpm), collected, and covered with ethanol, pH 10.5-11.0 (0.5-0.7 g KOH/L ethanol). The sample was boiled using a backflow condenser for 30 min. Then the alcohol was removed, the biomass was covered with 86% ethanol and separated from alcohol by centrifuging. In the next stage, the partly destroyed and defatted biomass was covered with chloroform and boiled for 30-40 min using a water bath with a backflow condenser. The sample was cooled and placed into a funnel to separate the chloroform extract of the polymer from the biomass. After separation of the phases, the polymer was precipitated by adding ethanol as a reagent. The procedure of re-dissolution and further precipitation of polymers was repeated several times to prepare specimens that would not contain organic impurities of protein, carbohydrate or lipid nature. All the organic solvents used in the procedure were preliminarily distilled to remove impurities.

2.4. Preparation and investigation of polymer films

High-purity PHA specimens were prepared as films and aqueous extracts and examined before testing. The films were prepared as follows: 2% polymer solutions in dichloromethane were cast in degreased Teflon-coated molds, and then the films were left to stay in a laminar flow cabinet (Labconco, U.S.) for 72 h until complete solvent evaporation took place. Aqueous extracts were prepared by soaking films in distilled water (1 mg : 1 ml) for 3 d at a temperature of 37°C. Distilled water maintained at the same temperature was used as the control.

The thickness of the films was measured with a LEGIONER EDM-25-0.001 electronic digital micrometer (Legioner, China).

The surface structure of the polymer films was examined using scanning and atomic-force electron microscopies. Prior to microscopy, 5×5 samples were sputter coated with platinum (at 10 mA, 3×20 s), with an Emitech K575X sputter coater (Quorum Technologies Limited, U.K.). SEM images were obtained using an S5500 electron microscope (Hitachi, Japan).

The roughness of film surface was determined using atomic-force microscopy (AFM) in semicontact mode (Integra Aura, NT-NDT, Russia). The arithmetic mean surface roughness (Ra) and the root mean square roughness (Rq) were determined based on 10 points, as the arithmetic averages of the absolute values of the vertical deviations of the five highest peaks and lowest valleys from the mean line of the profile of the surface, using conventional equations. Sites of areas 20 × 20 μm were examined, and 2 × 2 μm sites with local maxima and minima were selected; they were analyzed at a higher resolution, and the roughness of each sample was calculated as the average of three measurements.

The properties of film surfaces were determined by measuring water contact angles using a drop shape analyzer (Krüss, Germany) and software DSA-4 for Windows [24].

Films were cut into disks of 10 mm diameter, using a mold cutter. The samples were packed using an NS 1000 shrink-wrapping machine (Hawo Gmbh, Germany) and sterilized with H_2O_2 plasma in the Sterrad NX system (Johnson & Johnson, U.S.) for 45 min.

2.5. A study of hemocompatible properties of PHAs

To establish whether the PHA films can be used in contact with blood, we determined blood parameters (hemoglobin, hemolysis) and cell response to the contact with the film surface (erythrocytes, platelets, monocytes). Free hemoglobin was determined spectrophotometrically, using the Harboe assay [25]. The hemolytic effect of the aqueous extracts of all PHA types vs. sterile water was investigated in the *in vitro* experiments with isolated rabbit erythrocytes. The method was based on comparing the optical density of the suspension of aqueous extracts with blood at 530-550 nm and the optical density of the solution under 100% hemolysis; isotonic saline was used in the control. The quantitative criterion of the method was the percent hemolysis (α_h) determined using the following formula:

$$(\alpha_h) = \frac{D_x - D_c}{D_{100} - D_c} 100\%$$

where D_x is optical density of the sample incubated with the test material;

D_c is optical density of the control sample (negative control);

D_{100} is optical density of the sample after 100% hemolysis (positive control). The relative error was 10-15% at a confidence level of 0.95.

Erythrocytes were isolated from whole blood and erythrocyte mass of healthy donors, platelets – from donors' whole blood and platelet concentrate [3], and monocytes – from donors' peripheral blood in the density gradient of ficoll-urografin by the method of Recalde [26]. Determination of the number of attached cells and proportions of the main morphological types of erythrocytes included normal, damaged, and dead cells (% of the total).

Platelets attached to the surface of polymer films were counted and their morphology was studied using scanning electron microscopy (SEM S5500 Hitachi, Japan). Based on morphological changes, the platelets attached to the polymer film surfaces were divided into four classes, using a well-known method [20] : 1 – non-activated and non-deformed platelets;

2 – platelets with pseudopodia; 3 – fully spread platelets; 4 – aggregates. Total platelets attached to the surface of the films fabricated from four PHA types and the cells of each class were counted and compared to the control (high-density polyethylene, PE). For each sample, the numbers of cells in all fields were summed, and the relative index of platelet adhesion (RIPA) was calculated using the following formula:

$$RIPA = N_{Sample}/ N_{Control},$$

where N_{sample} and $N_{Control}$ are the number of cells on the sample and on the control (PE), respectively. RIPA values were also calculated for each platelet class: $RIPA_i$ (i = 1, 2, 3, 4). The relative error was 10% at a confidence level of 0.9.

Monocytes (MN) were isolated in the hypertonic density gradient of ficoll-verografin by the method of Recaldo [26]. The preliminarily prepared leukocyte mass was layered over the hypertonic gradient (specific density 1.080 g/cm^3) and centrifuged at 400 *g* for 15 min. The interphase MN fraction was washed twice with phosphate-buffered saline (pH=7.0) (Sigma-Aldrich (Merck), U.S.) and centrifuged at 400 *g* for 10 min. Cell concentrations were determined in Goryaev’s chamber. The cells were suspended in the DMEM medium (Thermo Fisher Scientific, U.S.) supplemented with 10% fetal bovine serum (FBS) (Thermo Fisher Scientific, U.S.), and cell concentration was adjusted to 2×10^6 cells/ml (10^5 cells in 50 µl).

Disks of films of PHAs with different compositions were placed into the wells of the 96-well culture plates (Sigma-Aldrich (Merck), U.S.), and 100 µl of the DMEM medium supplemented with 10% FBS and 50 µl of cell suspension (10^5 cells per well) were added. Culture plate plastic was used as the control. Monocytes were cultivated in a CO_2 incubator (Eppendorf (NBS), Germany) for 6 d. At Day 6, culture filtrates were collected.

Upon completion of cell incubation, culture medium was removed from the wells, and cells were fixed with 2.5% glutaraldehyde (Panreac, Spain) on the phosphate-buffered saline (Sigma-Aldrich (Merck), U.S.) for 2 h. Then, the cells in the wells were additionally fixed with 0.1% OsO_4 (Sigma-Aldrich (Merck), U.S.) for 40 min. The cell samples were washed and passed through a series of alcohols of ascending concentrations (10% to 100% ethanol in increments of 10%). PHA polymer disks were taken out of the wells (the bottom of the wells was cut out in the control) and mounted on aluminum supports or metallic sample stages. The samples were sputter coated with platinum in a sputter coater (Emitech K575XD) in three cycles, 20 s each, with the 10 mA current, and analyzed using a TM 3000 microscope (HITACHI, Japan). X-ray spectral analysis was performed using the Quantax 70 software.

Viable monocytes were determined in the MTT assay.

At the end of the incubation, the culture medium was removed from the wells, and the cells were washed with fresh DMEM medium with 10% FBS. 200 μl of MTT solution (Sigma-Aldrich, U.S.) in DMEM medium with 10% FBS (final MTT concentration 0.25 mg/ml) was added to the wells. The cells were incubated for 4 h. After the incubation, the medium was replaced by 150 μl of DMSO (Amresco, USA). Aliquots of 100 μl were transferred to clean plates and the optical density was determined at $\lambda = 550$ nm on a multichannel reader iMark™ Microplate Absorbance Reader (Bio-Rad, U.S.).

2.4. Statistics

The results were analyzed statistically using the standard software package of Microsoft Excel, STATISTICA 8. Arithmetic means and errors of the arithmetic means were calculated, depending on the sample size, using the Mann-Whitney U test and Student' *t*-test (significance levels: 0.05 and 0.01). Results were given as X±m.

3. Results and discussion

3.1. Synthesis and characterization of different PHAs

Microorganisms capable of synthesizing PHAs with different compositions can be used to produce polymers with tailored properties. Bacterial culture in the mode of synthesis of PHA copolymers is a complex and multifactor system, which is controlled by various parameters. Firstly, PHA synthesis occurs under the conditions prohibiting deficiency in the main carbon substrate, and substrate concentration must be controlled within the range of its physiological effect on the cultivated strain, preventing the establishment of either limiting or inhibiting conditions. Secondly, to achieve PHA accumulation, for most producers, one of the substrates of constructive metabolism (nitrogen, phosphorus, etc.) must limit cell growth. Thirdly, the culture medium must contain a precursor substrate, and its concentration must be sufficient to enable formation of the monomers other than 3HB (3HV, 4HB, or 3HHx) but not high enough to cause serious inhibition of the cells. Fourthly, an important fact is that PHA, being substrate of endogenous respiration, is metabolized intracellularly by intracellular depolymerases. Carbon chains are broken down, and monomers with the chains composed of more than 4 carbon atoms are depolymerized and are then involved in PHA resynthesis as shorter monomers, mainly 3-hydroxybutyrate. Hence, the fractions of monomers other than 3HB in PHA are decreased.

Production of PHAs with different chemical composition was achieved by cultivating cells under nitrogen deficiency in the culture medium, specific conditions of carbon supply, and dosed feeding of precursor substrates of 4HB, 3HV, and 3HHx and by collecting samples at proper time moments after precursor substrate feeding events. The PHAs produced included a monomer of homopolymer of 3-hydroxybutyric acid $[–O–CH(CH_3)–CH_2–CO–]_1$ [P(3HB)]; a copolymer of 3-hydroxybutyric and 4-hydroxybutyric acids $[–O–CH_2–CH_2–CH_2–CO–]_2$ [P(3HB/4HB]; a copolymer of 3-hydroxybutyric and 3-hydroxyvaleric acids $[–CH(C_2H_5)–CH_2–CO–]_3$ [P(3HB/3HV)]; and a copolymer of 3-hydroxybutyric and 3-hydroxyhexanoic acids $[–O–CH(C_3H_7)–CH_2–CO–]_4$ [P(3HB/3HHx)]. 3HB monomers were the major components of all copolymers, and the contents of the second monomers were similar to each other (10.0±0.5 mol.%) (Table 1).

Although the contents of 3HV, 4HB, and 3HHx monomers in PHAs were rather low (about 10 mol.%), the PHA specimens had different properties. The weight average molecular weights (M_w) of all copolymers were significantly lower than the molecular weight of P(3HB): 550-676 kDa and 920 kDa, respectively. In addition, the copolymers had higher polydispersity (above 3) than the homopolymer – 2.12. The T_{melt} and T_{degr} of copolymers were generally 10-15°C lower than the corresponding temperatures of the homopolymer. The copolymers showed a more pronounced decrease in the glass transition temperature than P(3HB), but the difference between the T_{melt} and T_{degr} was at least 100-110°C in all specimens – an important property for melt processing of the polymers. The copolymers differed significantly in their degrees of crystallinity, which decreased from P(3HB-co-3HV) to P(3HB-co-3HHx) to P(3HB-co-4HB). The C_x of copolymers containing 4-hydroxybutyrate and 3-hydroxyhexanoate monomers was 50% lower. Thus, incorporation of other monomers into the carbon chain of 3-hydroxybutyrate caused the amorphous and crystalline regions in the polymer to become nearly equal to each other, resulting in a lower degree of crystallinity. These results generally agree with the available literature data [27-29].

It is difficult to compare quantitative evaluations of PHA properties, as the data obtained by different authors vary considerably. For instance, the difference between the data reported on the molecular weight of P(3HB) may reach two orders of magnitude [28]. The data on the degrees of crystallinity of PHAs with different chemical compositions are scant and rather contradictory. P(3HB-co-3HV) containing up to 20–22 mol.% 3HV was found to have a high degree of crystallinity (70-80%) [30]; in another study [31], however, the polymer of a similar composition had very low C_x (5-9%). The C_x of P(3HB-co-3HHx) containing 12–18 mol.% 3HHx was 38–40% [31], but Fukui T. et al. [32] reported a similar degree of crystallinity for the polymer that contained much lower 3HHx (1.5 mol.%). The melting point (T_{melt}) and thermal degradation temperature (T_{degr}) of the PHA are very important parameters, which determine the conditions of its melt processing. The T_{melt} of P(3HB) reported by different authors ranged between 162 and 197°C. The values of T_{melt} reported for P(3HB-co-3HV) vary considerably. For instance, for the polymer containing 6 mol.% 3HV, the T_{melt} was determined as 186°C, but a similar specimen in another study had the T_{melt} of 170°C. Even more contradictory data are reported for the T_{melt} of P(3HB-co-4HB): for the specimens with similar contents of 4HB, 2 to 7 mol.%, the melting points were found to vary between 114 and 172°C [28]. The reason for the inconsistencies in the data on the properties of PHAs produced by different authors at different time is that the PHAs were synthesized by different producers in different media. The PHA specimens could differ in the amounts of residual impurities (e.g., lipids) and processing techniques employed. Finally, the authors used dissimilar methods in their studies.

3.2. Characterization of polymer films

The film thickness (average of 10 measurements) was 25 μm (the error was 0.026). Segments of equal thickness were selected and disks of diameter 10 mm were cut out to be further used in the experiments

SEM images of the films prepared from PHAs with different chemical compositions, degrees of crystallinity, and, hence, crystallization kinetics showed dissimilarities in their surface microstructure (Figure 1). The surfaces of the films of the homopolymer P(3HB) were the smoothest, dense, and almost pore-free. On the surface of the films prepared from low-crystallinity copolymers P(3HB-co-4HB) and P(3HB-co-3HHx), there were numerous large, 5-8-nm, pores. On the surface of the P(3HB-co-3HV) films, there were distinct folds and a few 3-5-nm pores.

An important parameter determining biocompatibility of implants is physicochemical reactivity of their surface. The main factors that influence protein adhesion, cell attachment, and response of the surrounding tissues are surface topography, chemical composition, and phase composition. The nanometer surface roughness can affect cell adhesion, spreading, and motility and influence the synthesis of specific proteins.

AFM examination of the surface of PHA films showed that the three types of copolymer films had similar values of the arithmetic mean surface roughness (Ra) and the root mean square roughness (Rq): 158-177 and 198-248 nm, respectively. Those values were considerably higher than the Ra and Rq obtained for P(3HB) films: 71 and 80 nm, respectively (Figure 2, Table 2). Hence, the presence of the monomers other than 3-hydroxybutyrate in the PHA was an essential factor in the development of film topography.

Results obtained in the present study are consistent with the literature data suggesting that the composition of the monomers in the PHA influences the surface microstructure of the films produced from the polymer. Atomic force microscopic analysis showed that surface roughness values of all films from P(3HB-co-3HV) with 26 and 12 mol.% HV was 92.5 and 290.8 nm, rising to 588.8 nm when polyethylene glycol was added [33]. A study by Bera et al.[34], like the present study, showed that incorporation of 3HV monomers into the P(3HB) chain increased the surface roughness of the films. However, other data suggested that an increase in the molar fraction of 4HB in P(3HB-co-4HB) resulted in lower roughness of film surface [35-37]. The surface of P(3HB-co-3HHx) films was described as smoother than the surface of the films based on the P(3HB-co-4HB-co-3HHx) terpolymer [38]. Even small changes in surface topography can lead to variations in cellular response within a wide range – from a slight increase to a considerable inhibition of cellular activity. This effect is, however, specific, and cells differ in their sensitivity to variations in the surface roughness and topography.

A major parameter that indirectly characterizes biological compatibility of the material and influences cell adhesion and viability is hydrophilic/hydrophobic balance of the surface. This balance is expressed as water contact angle. Being hydrophobic, P(3HB) is not the material of choice for constructing medical implants, as it does not facilitate cell adhesion. Because of their hydrophobic properties, the biocompatibility associated with PHAs is found to be inadequate [39]. Various approaches can be used to enhance hydrophilicity of PHAs: blending them with other materials, chemical surface modification, laser cutting, and biosynthesis of polymers with different compositions, mainly copolymers.

The measurements showed that P(3HB) films had the largest contact angle (70.0±0.4°) (Table 2). Films prepared from PHA copolymers had lower values of water contact angle, suggesting that incorporation of monomers other than 3-hydroxybutyrate into the PHA enhanced hydrophilicity of the material. The P(3HB-co-3HV) and P(3HB-co-3HHx) films showed similar values of water contact angle (60.0-62.5°), and they were comparable to the water contact angle of polystyrene culture plates. The films of P(3HB-co-4HB), which had the lowest degree of crystallinity (C_x), showed the lowest values of water contact angle (57.4±0.6°). That was an intermediate region between hydrophobic and hydrophilic surfaces. Surface energy is another parameter that can affect behavior of cells. P(3HB) films, which were the least hydrophilic, had the lowest surface tension (32.8 erg/cm^2) (Table 2). The surface tension values of all copolymer films were at least 10-13 erg/cm^2 higher. A number of studies reported approaches to increasing PHA hydrophilicity such as synthesis of polymers with a longer carbon chain (so-called medium-chain-length polymers, including copolymers with 3HHx and generation of branched side chains), production of PHA blends and hybrids with such agents as polyethylene glycol [40-41].

3.3. A study of hemocompatible properties of PHAs

Hemocompatible materials in contact with blood must not induce thromboses, thromboembolisms, antigenic response, destruction of blood constituents and plasma proteins, etc. [42]. An indicator of hemocompatibility of biomaterials is the state of the hemostasis system; the morphology of adhering platelets [43, 44], monocyte reactions, complement activation [45], and others [1].

The differences revealed in the surface structure and properties of the PHAs with different chemical compositions did not produce any adverse effects on the morphological/functional properties of blood cells. Contact with polymer films of all PHA types did not cause any impairment of the biological properties of blood cells. None of the specimens produced adverse effects on erythrocytes; the number of damaged erythrocytes did not increase after contacting polymer films. The best parameters in terms of the types of the altered and damaged erythrocytes were obtained on films made from P(3HB-co-4HB) and P(3HB-co-3HHx) (Table 3).

Hemoglobin content in the blood that was in contact with the PHA films did not change either. Hemolysis assay showed that none of the PHA extracts caused hemolysis. None of the PHA extracts produced a hemolytic effect on erythrocytes; the hemolytic activity in the treatments was 0.06-0.10 (the maximum acceptable level being 2%).

In a study by Youxi Zhao, hemolysis rate was no higher than 4% for all tested PHB and PHBV. That was well within the limit of 5% hemolysis, which is permissible for biomaterials [46]. The hemolysis rate on the PHBV-B film was close to that of the control sample, while it was the lowest for PHBV-H [47].

Important results were obtained in the study of platelets. These cells are very sensitive to changes in their environment and easily damaged. Moreover, platelets readily adhere to various materials, including biomaterials. The adhesion of platelets to PHA films was insignificant (below 0.01 thousand cells per 1 cm^2), and no platelet activation or damage was observed. That is, platelet adhesion should be interpreted as passive sticking/adsorption of cells, which was not associated with their adhesive activity. Quantitative analysis of platelet adhesion on the film surface (determination of $RIPA_i$) was performed for each PHA type (Figure 3).

It has been generally accepted that morphology of platelets changes during their activation: round cells are considered as non-activated platelets, while the cells with pseudopodia and spread cells are regarded as activated platelets. The morphology of platelets (the activated to non-activated cell ratio) constituting aggregates varied significantly on films with different topographies (Fig. 4). On the copolymer films, the aggregates mainly consisted of non-activated round platelets, while on P(3HB) and PE films, the platelets constituting aggregates were dominated by activated forms (platelets with pseudopodia) (Fig. 3, 4).

The total number of non-activated platelets attached to the surfaces of all PHA films was 1.5-2.2 times lower than the number of cells in the control (on high-density polyethylene). The best results were obtained for the films made from the low-crystallinity P(3HB-co-4HB) and P(3HB-co-3HHx). The number of the spread platelets, platelets with pseudopodia, and aggregates was lower on all PHA films compared to PE. These data suggest that the experimental specimens showed good hemocompatibility at the stage of cell response (platelet response to foreign surface). No significant changes were revealed in the morphology of the platelets attached to the surfaces of all the experimental specimens. The most favorable films for platelet contact were the films prepared from the low-crystallinity P(3HB-co-4HB) and P(3HB-co-3HHx), which had the most hydrophylized surface. This result was consistent with the data reported in another study [20], in which the authors showed that platelet response was weaker on contact with PHA films than in the control (on high-density polyethylene), and the counts of attached and non-activated platelets were higher on films of P(3HB-co-3HV) compared to P(3HB) films.

Generally, surface characteristics, especially wettability and surface energy of the biomaterial surface, play a crucial role in the adhesion and activation of platelets on the surface, which serves as an important step in thrombosis [46]. A material with high surface energy leads to stronger interactions with water and consequently will be more wettable.

Thus, with the decrease in surface energy of a material, its hydrophobicity generally increases. Comparable data were reported in a study by J. Han 2015. The authors of that study investigated hemolysis and adhesion of rabbit blood platelets on films of two PHA types. P(3HB) and P(3HB-co-3HV) films showed high hydrophobicity (78±0.92º) and lower surface free energy (32.8 erg/cm^2). Those favorable surface properties of that biomaterial caused high platelet adhesion, platelet activation, and fast blood coagulation [48].

Platelet activation is associated with the increase in the activity of NADPH-dependent oxidases and a rise in the production of reactive oxygen species: induction of oxidative stress – the basis of thromboses under physiologically normal conditions and under pathogenesis [49]. Thus, the increase in the reduction rate of formazan in MTT assay can be used as an indicator of oxidative stress (Fig. 5).

Results of MTT assay showed that formazan production rate varied considerably on films with different surface topographies (Fig. 5), suggesting that surface topography can "control" the rate of generation of free oxygen species and the level of oxidative stress in platelets. Thus, the highest activation of platelets by the surface topography was achieved on films of low-crystallinity polymers, P(3HB-co-4HB) and P(3HB-co3HHx).

Unfortunately, results obtained for erythrocytes and platelets cannot be compared with the literature data, as there are no available studies reporting similar investigations.

Particular consideration was given to the response of monocytes to polymer films of different compositions: these blood cells play a major role in the body's immune response to damaging factors, including foreign body reaction. Monocytes are precursors of macrophages and the largest and most active phagocytes of peripheral blood, which are capable of consuming relatively large particles and cells without dying after performing phagocytosis, unlike microphages (neutrophils and eosinophils). Activated monocytes and tissue macrophages are responsible for antitumor, antiviral, antimicrobial, and antiparasitic immunity, producing cytokines, interleukin, and interferon; they take part in regulation of hematopoiesis and formation of the body's specific immune response. Macrophages play a particularly important role when bioresorbable devices are implanted, as they are involved in resorption of the implants [12]. Subpopulations of monocytes are labile systems, whose abundance and functional activity may vary considerably under physiologically normal conditions and under pathogenesis [49].

Monocytes were cultivated on films of PHAs with different compositions and with different surface topography to study their response and morphology compared to the control (culture plate plastic). Morphological analysis revealed two main morphological classes of monocytes: Class 1 – round immobile cells; Class 2 – elongated mobile cells (Figure 6) [50]. Both morphological classes were observed in cultures on PHA films and on culture plate plastic. However, the elongated to round (mobile to immobile) cell ratio varied considerably depending on the chemical composition of the films, which differed in their surface structure (Figure 7). The largest motile and physiologically active monocytes were observed on P(3HB-co-4HB) and P(3H-co-3HHx) films; they constituted 55-64%, and that was 1.2-1.5 times higher than on P(3HB) and in the control.

Under in vitro conditions, the ratio of the two morphological classes, elongated cells (Ec) and round cells (Rc), can be used to estimate the direction of the M1/M2 processes of MN polarization: round cells are associated with the M1 phenotype (pro-inflammatory macrophages), and elongated cells are associated with the M2 phenotype (anti-inflammatory macrophages, taking part in repair processes [51,52]. Therefore, the variations in the counts of the two morphological classes on different polymer films may be caused by the effect of the surface topography on dynamics of macrophage polarization processes. The topography of the low-crystallinity copolymers containing 4HB and 3HHx was favorable for the increase in the number of mobile cells and the increase in the number of MuNC.

Thus, the abundances of various morphotypes of elongated, motile macrophages were greater on the copolymer scaffolds, which showed higher hydrophilicity, porosity, and roughness than the films of pure P(3HB). Morphotypes of elongated cells exhibit mesenchymal mode of migration [53]. Round cells exhibit amoeboid migration [54, 55]. The mesenchymal and amoeboid modes of migration are related to different types of intracellular signaling [53]. The different proportions of the round and elongated morphological types on films made of different polymers suggest that the features of the surface topography chiefly activate one of the types of intracellular signaling and determine the mode of the locomotor activity of macrophages. The literature data indicate that the structure and properties of the scaffolds influence the morphology and functional activity of monocytes/macrophages in vitro. Studies of poly(ε-caprolactone)-scaffolds [56] and polydioxanone-scaffolds [57] showed that increased hydrophilicity and elasticity exerted favorable effects on this type of cells.

Thus, none of the film types negatively affected the blood cells examined in the present research. Films prepared from polymers differing in the degree of crystallinity varied considerably in the properties influencing hemocompatibility of the material: the ratio of the crystalline to amorphous regions (degree of crystallinity), surface development, hydrophobic/hydrophilic balance, porosity, and elasticity. The physicochemical properties of a material largely determine its bio- and hemo-compatibility, which can be achieved by forming a mixed phase with a high degree of nanoscale heterogeneity in the polymer bulk, caused by the strong association between “soft” and “hard” segments and the sizes of the crystalline and amorphous phases [1, 58].

This is consistent with the results of the present study, which shows that films of the low-crystallinity P(3HB-co-4HB) and P(3HB-co-3HHx), which have the highest hydrophilicity and roughness, are the most favorable for erythrocytes, platelets, and monocytes.

Conclusion

Four types of PHAs with different contents of 3HV, 4HB, and 3HHx monomers (about 10 mol.%) were synthesized using the strain *Cupriavidus eutrophus* B10646 cultivated under the previously developed conditions of autotrophic and heterotrophic growth. All copolymers had reduced weight average molecular weights (M_w) and degrees of crystallinity – about 550-676 kDa and 42-64% – compared to the homopolymer. Thus, films prepared from four PHA types, which had different chemical compositions, did not cause unfavorable responses of erythrocytes, platelets, and monocytes, as suggested by results of the study of their parameters. Films prepared from low-crystallinity copolymers, containing 4-hydroxybutyrate and 3-hydroxyhexanoate monomer units, were the most favorable for cells. Those polymers had the lowest degree of crystallinity, and films made of them were the most hydrophilic, with the most porous and developed surface. They should be tested in further studies as materials for constructing blood-contacting implants.

Declaration of Conflicting Interests

The author(s) declared no potential conflicts of interest with respect to the research, authorship, and/or publication of this article.

Funding

The author(s) disclosed receipt of the following financial support for the research, authorship, and/or publication of this article: The study is supporting by the Russian Science Foundation, Project No 17-15-01352

References

[1] V. Sevastyanov, Biocompatible materials, LLC Publishing House Medical Information Agency, Moscow, 2011.

[2] L. Kokov, Vascular and intraorgan stenting, Graal, Moscow, 2003.

[3] J. Zidar, M. Lincoff, R. Stack, Biodegradable stents, in: J. Zidar, Textbook of Interventional Cardiology, 2nd ed. Saunders, Philadelphia, 1994, pp.787–802.

[4] A. Carroccio, S. Ellozy, D. Spielvogel, Endovascular Stent Garfting of Thoracic Aortic Aneurysms, Ann. Vasc. Surg. 17 (2003) 473–478. https://doi.org/10.1007/s10016-003-0026-x

[5] C.R. Conti. Restenosis. Restenosis after angioplasty: Have we found the Holy Grail?, Clin. Cardiol. 25 (2002) 47–48.

[6] M.T. Costagna, G.S. Mintz, B.O. Leiboff, J.M. Ahmed, R. Mehran, L.F. Satler, K. M. Kent, A.D. Pichard, N.J. Weissman, The contribution of “mechanical” problems to in-stent restenosis. An intravascular ultrasound analysis of 1090 consecutive in-stent restenosis lesions, J. Amer. Heart. 142 (2001) 970–974. https://doi.org/10.1067/mhj.2001.119613

[7] Q. Liu, C. Tieche, P. Alkema, Neointima formation on vascular elastic laminae and collagen matrices scaffolds implanted in the rat aortae, Biomaterials. 25 (2004) 1869–1882. https://doi.org/10.1016/j.biomaterials.2003.08.044

[8] H. Tamai, K. Igaki, E. Kyo, K. Kosuga, A. Kawashima, S. Matsui, H. Komori, T. Tsuji, S. Motohara, H. Uehata, Initial and 6-month result of biodegradable poly-L-lactic acid coronary stents in humans, Circulation. 102 (2000) 399–404. https://doi.org/10.1161/01.CIR.102.4.399

[9] T. Tsuji, H. Tamai, K. Igaki, E. Kyo, K. Kosuga, A. Kawashima, S. Matsui, H. Komori, S. Motohara, H. Uehata, and E. Takeuchi, Biodegradable stents as a platform to drag

loading, Int. J. Cardiovasc. Intervent. 5 (2003) 13–16. https://doi.org/10.1111/j.1540-8183.1999.tb00673.x

[10] A. Wong, C. Chan, Drug-eluting stents: the end of restenosis?, Ann. Acad. Med. Singapore, 33 (2004) 423–431.

[11] R. Wessely, A. Shoming, A. Kasrati, Sirolomus and Paclitaxel on Polymer-Based Drug-Eluting Stents, J. of American College of Cardiology, 47 (2006) 48–53. https://doi.org/10.1016/j.jacc.2005.09.047

[12] T.G. Volova, Polyoxyalkanoates are biodegradable polymers for medicine. SB RAS, Novosibirsk, 2006.

[13] K. Sudesh, Practical Guide to Microbial Polyhydroxyalkanoates, SY4 4NR, United Kingdom, 2010.

[14] T. Volova, E.Shishatskaya, Biomedical studies of PHAs produced in the Institute of Biophysics SB RAS and Siberian Federal University. In: L.P. Wu (Eds.), Polyhydroxyalkanoates (PHA): Biosynthesis, Indastrial Production and Applications in Medicine, Nova Scienses Publ., New York, 2014, p.273–330.

[15] T.G. Volova, Y.S. Vinnik, E.I. Shishatskaya, Natural-based polymers for biomedical applications, Appl Acad Perss, Canada, 2017.

[16] A.K. Singh, J.K. Srivastava, A.K. Chandel, Sharma, N. Mallick, S.P. Singh, Biomedical applications of microbially engineered polyhydroxyalkanoates: an insight into recent advances, bottlenecks, and solutions, Appl. Microbiol. Biotechnol., 103 (2019) 2007–2032. https://doi.org/10.1007/s00253-018-09604-y

[17] A.A. Shumilova, M.P. Myltygashev, A.K. Kirichenko, E.D. Nikolaeva, T.G. Volova, E.I. Shishatskaya, Porous 3D implants of degradable poly-3-hydroxybutyrate used to enhance regeneration of rat cranial defect, J. Biomed. Mater. Res. A. 105 (2017) 566–577. https://doi.org/10.1002/jbm.a.35933

[18] G. Zinner, D. Behrend, K.P. Schmitz, The hemostasis system as an indicator of hemocompatibility of implantant materials, Biomed. Tech. 43 (1998) 432–433.

[19] G. Zinner, D. Behrend, K.P. Schmitz, Complement activation and libaration of cytokines from monocytes as indicators of biocompatibility of polyhydroxybutyric acid, Biomed. Tech. 42 (1997) 55–56.

[20] V.I. Sevastianov, N.V. Perova, E.I. Shishatskaya, G.S. Kalacheva, T.G. Volova, Production of purified polyhydroxyalkanoates (PHAs) for applications in contact with blood, J. Biomater. Sci. Polymer. Edn. 14 (2003) 1029–1042. https://doi.org/10.1163/156856203769231547

[21] L.S. Kokov, A.N. Balan, A.V. Pokrovsky, The first experience of the clinical use of the domestic nitinol stent for the treatment of stenotic lesions of arteries, Angiology and Vascular Surgery, 4 (1999) 20–24 [Russia].

[22] A.V. Protopopov, E. P. Konstantinov, E.I. Shishatskaya, Use of resorbable polyesters to enhance biocompatibility of vascular stents, Technology of living systems. 5 (2008) 25–34 [Russia].

[23] T.G. Volova. Strain bacteria Cupriavidus eutrophus VKPM B-10646 is producer polyhydroxyalkanoates and methods for their production. Patent 2439143, Russia, 2012.

[24] D. K. Owens, R. C. Wendt, Estimation of the surface free energy of polymers, J. Appl. Polym. Sci. 13 (1969) 1741–1747.

[25] M.A. Harboe, Method for determination fhe moglobinin plasma bynear-ultraviolet spectrophotometry, Scand. J. Clin. Lab. Invest. 11 (1959) 66–70.

[26] H.R. Recaldo. A simple method of obtaining monocytes in suspension, J. Immunol. Methods. 69 (1984) 71–77.

[27] K. Sudesh, H. Abe, Y. Doi Synthesis, structure and properties of polyhydroxyalkanoates: biological polyesters, Progress in Polymer Science. 25 (2000) 1503–1555. https://doi.org/10.1134/S0026261708030119

[28] B. Laycock, P. Halley, S. Pratt, A. Werker, P. Lant, The chemomechanical properties of microbial polyhydroxyalkanoate, Prog. Polym. Sci. 38 (2013) 536–583. https://doi.org/10.1016/j.progpolymsci.2012.06.003

[29] S.P. Singh, Janmejai Kumar Srivastava, A. K. Chandel, L. Sharma, N. Mallick, Biomedical applications of microbially engineered polyhydroxyalkanoates: an insight into recent advances, bottlenecks, and solutions, Appl. Microbiol. Biotech. 103 (2019) 2007–2032. https://doi.org/10.1007/s00253-018-09604-y

[30] I. Noda, P. R. Green, M.M. Satkowski, L.A. Schechtman, Preparation and properties of novel class of polyhydroxyalkanoate copolymers, Biomacromolecules, 6 (2005) 580–586. https://doi.org/10.1021/bm049472m

[31] Y. Dai, Z. Yuan, K. Jack, J. Keller, Production of targeted poly(3-hydroxyalkanoates) copolymers by glycogen accumulating organisms using acetate as sole carbon source, J. Biotechnol. 129 (2007) 489–497. https://doi.org/10.1016/j.jbiotec.2007.01.036

[32] T. Fukui, H. Abe, Y. Doi, Engineering of Ralstonia eutropha for production of poly(3-hydroxybutyrate-co-3-hydroxyhexanoate) from fructose and solid-state properties of the copolymer, Biomacromolecules. 3 (2002) 618-624. https://doi.org/10.1021/bm0255084

[33] V.A. Surguchenko, A.S. Ponomareva, A.E. Efimov, E.A. Nemets, I.I. Agapov, V.I. Sevastianov, Characteristics of adhesion and proliferation of mouse NIH/3T3 fibroblasts on the poly(3-hydroxybutyrate-co-3-hydroxyvalerate) films with different surface roughness values, Messenger of Transplantology and Artifi cial Organs. 41 (2012) 72–77. . https://doi.org/10.15825/1995-1191-2012-1-72-77

[34] A.Bera, S.Dubeyb,K.Bhayanib, D.Mondala, S.Mishra, P. K.Ghoshab, Microbial synthesis of polyhydroxyalkanoate using seaweed-derived crude levulinic acid as co-nutrient, International Journal of Biological Macromolecules, 72 (2015) 487–494. https://doi.org/10.1016/j.ijbiomac.2014.08.037

[35] S. Chanprateep, K. Buasri, A. Muangwong et al. Biosynthesis and biocompatibility of biodegradable poly(3-hydroxybutyrate-co-4-hydroxybutyrate), Polymer Degradation and Stability, 95 (2010) 2003–2012.

[36] J. Zhang, Q. Cao, S. Li, X. Lu, Y. Zhao, J.S. Guan, J.C. Chen, Q. Wu, G.Q. Chen, 3-Hydroxybutyrate methyl ester as a potential drug against Alzheimer's disease via mitochondria protection mechanism, Biomaterials, 34 (2013) 7552–7562. http://dx.doi.org/10.1016/j.biomaterials.2013.06.043

[37] J. Zhang, E.I. Shishatskaya, T.G. Volova, L.F. da Silva, G.Q. Chen. Polyhydroxyalkanoates (PHA) for therapeutic applications, Mater. Sci. Eng. C Mater. Biol. Appl. 86 (2018) 144–150. https://doi.org/10.1016/j.msec.2017.12.035

[38] D.X. Wei, J.W. Dao, G.Q. Chen. A micro-ark for cells: highly open porous polyhydroxyalkanoate microspheres as injectable scaffolds for tissue regeneration, Adv. Mater. (2018) 1–11.

[39] X. Yang, K. Zhao, G.Q. Chen. Effect of surface treatment on the biocompatibility of microbial polyhydroxyalkanoates, Biomaterials, 23 (2002) 1391–1397. https://doi.org/10.1016/S0142-9612(01)00260-5

[40] Q. Cao, J. Zhang, H. Liu, Q. Wu, J. Chen, G.Q. Chen, The mechanism of anti-osteoporosis effects of 3-hydroxybutyrate and derivatives under simulated microgravity, Biomaterials. 35 (2014) 8273–8283.

[41] H. Ye, K. Zhang, D. Kai, Z. Li, X.J. Loh, Polyester elastomers for soft tissue engineering, Chem. Soc. Rev. 47 (2018) 4545–4580. http://dx.doi.org/10.1039/c8cs00161h

[42] V.I. Sevastianov, A Comprehensive Guide to Medical and Pharmaceutical Applications, in: M. Szycher (Eds.), High-Performance Biomaterials, Technomic Publ.Co., Pennsylvania, 1991, 245.

[43] V.I. Sevastianov, I.B. Rosanova, S.L.Vasin, E.A. Nemets, V.N. Vasilets, in: Biomaterials and Drug Delivery toward New Mellenium. p.497,

[44] K.D. Park, I.C. Kwon, N. Yui, S.Y. and K. Park. Yan Rim Won (Eds.). Publ. Co., Seoul, Korea, (2000)

[45] I.A. Titushkin, S.L. Vasin, I.B. Rozanova, E.N. Pokidyshva, A.P. Alekhin, V.I. Sevastianov, Influence of structural and energy properties of carbon coatings on adhesion of human platelets, ASAIO Journal. 11 (2001) 43–51.

[46] W.F. Ou, H.D. Qiu, Z.F. Chen, Biodegradable block poly (ester-urethane)s based on poly (3-hydroxybutyrate-co-4-hydroxybutyrate) copolymers, Biomaterials. 32 (2011) 3178–3188. https://doi.org/10.1016/j.biomaterials.2011.01.031

[47] Y. Zhao, Z. Rao, Y. Xue, P. Gong, Y. Jib, Y.Mac, Biosynthesis, property comparison, and hemocompatibility of bacterial and haloarchaeal poly(3-hydroxybutyrate-co-3-hydroxyvalerate), Science Bulletin. 60 (2015) 1901– 1910. https://doi.org/10.1007/s11434-015-0923-8

[48] J. Han, L.P. Wu, J. Hou, D. Zhao, H. Xiang, Biosynthesis, Characterization, and Hemostasis Potential of Tailor-Made Poly(3-hydroxybutyrate-co-3-hydroxyvalerate) Produced by *Haloferax mediterranei*, Biomacromolecules. 2 (2015) 578–88. doi: 10.1021/bm5016267

[49] M. Wildgruber, T. Aschenbrenner, H. Wendorf, M. Czubba, A. Glinzer, B. Haller, M. Schiemann, A. Zimmermann, H, Berger, H.H. Eckstein, R. Meier, W.A. Wohlgemuth, P.Libby, A. Zernecke, The “Intermediate” CD14++CD16+monocyte subset

increases in severe peripheral artery disease in humans, Scientific Reports, 6 (2016) 1–8. http://dx.doi.org/10.1038/srep39483.

[50] R.J. Miron, D.D. Bosshardt, E. Hedbom, Y. Zhang, B. Haenni, D. Buser, A.Sculean, Adsorption of enamel matrix proteins to a bovine-derived bone grafting material and its regulation of cell adhesion, proliferation, and differentiation, J. Periodontol, 83 (2012) 936–947. https://doi.org/10.1902/jop.2011.110480

[51] F. Rey-Giraud, M. Hafner, C.H. Ries, In vitro generation of monocyte-derived macrophages under serum-free conditions improves their tumor promoting functions, PLoS One 7(2012) 1–10. https://doi.org/10.1371/journal.pone.0042656

[52] F. Heinrich, A. Lehmbecker, B.B. Raddatz, K. Kegler, A. Tipold,V.M. Stein, A. Kalkuhl, U. Deschl, W. Baumgärtner, R. Ulrich, I. Spitzbarth, Morphologic, phenotypic, and transcriptomic characterization of classically and alternatively activated canine blood-derived macrophages in vitro, PLoS One. 17 (2017) 1–33. https://doi.org/10.1371/journal.pone.0183572

[53] E. Van Goethem, R. Poincloux, F. Gauffre, I. Maridonneau-Parini, V. Le Cabec, Matrix architecture dictates three-dimensional migration modes of human macrophages: differential involvement of proteases and podosome-like structures, J Immunol.184 (2010) 1049–1061. https://doi.org/10.4049/jimmunol.0902223

[54] E.K. Paluch, I.M. Aspalter, M. Sixt, Focal adhesion-independent cell migration, Annu Rev Cell Dev Biol. 32 (2016) 469–490. https://doi.org/10.1146/annurev-cellbio-111315-125341

[55] P.R. O'Neill, J.A. Castillo-Badillo, X. Meshik, V. Kalyanaraman, K. Melgarejo, N. Gautam, Membrane flow drives an adhesion-independent amoeboid cell migration mode, Dev Cell. 46 (2018) 9–22. https://doi.org/10.1016/j.devcel.2018.05.029

[56] Z. Wang, Y. Cui, J. Wang, X. Yang, Y. Wu, K. Wang, X. Gao, D. Li, Y. Li, X.L. Zheng, Y. Zhu, D. Kong, Q. Zhao, The effect of thick fibers and large pores of electrospun poly(epsiloncaprolactone) vascular grafts on macrophage polarization and arterial regeneration, Biomaterials. 35 (2014) 5700–5710. https://doi.org/10.1016/j.biomaterials.2014.03.078

[57] K. Garg, C.L. Ward, B.T. Corona, Asynchronous inflammation and myogenic cell migration limit muscle tissue regeneration mediated by a cellular scaffolds, Inflamm Cell Signal. 1(2014) http://dx.doi.org/10.14800/ics.530

[58] C. Siedlecki, Hemocompatibility of Biomaterials for Clinical Applications: Blood-Biomaterials Interactions, Woodhead Publishing, USA, 2018.

Figure 1. SEM images of the surface microstructure of the films prepared from PHAs with different chemical compositions: A – P(3HB), B – P(3H-co-4HB), C – P(3HB-co-3HV), D – P(3HB-co-3HHx)

Figure 2. AFM images of the surface roughness of the films prepared from PHAs with different chemical compositions

Figure 3. RIPA$_i$ values for the four classes of platelets attached to the surface of the polymer films of different compositions: I – PE (control); II – P(3HB); III P(3HB-co-4HB); IV – P(3HB-co-3HV); V – P(3HB-co-3HHx). Cell classes: 1 – non-activated platelets; 2 – platelets with pseudopodia; 3 – fully spread platelets; 4 – aggregates; 5 – total attached cells

Figure 4. Morphology of platelets after 24 h cultivation on the surface of the polymer films of different compositions: I – PE (control); II – P(3HB); III P(3HB-co-4HB); IV – P(3HB-co-3HV); V – P(3HB-co-3HHx).

Figure 5. Reduction of MTT to formazan in platelets after 24 h cultivation on polymer films with different surface topographies. I – PE (control); II – P(3HB); III P(3HB-co-4HB); IV – P(3HB-co-3HV); V – P(3HB-co-3HHx)

Figure 6. The main morphological classes of monocytes cultivated on the culture plate plastic (control) for 6 d: A, B – round immobile cells, Class 1; A – polyploid cell morphotype, B – diploid cell morphotype. C, D – elongated mobile cells, Class 2. C – spindle cell morphotype; relatively "short" cells with distinct spindle-like central thickening of the body. D – rod cell morphotype; elongated cells of nearly uniform diameter. E – filamentous cell morphotype; very long, "thin" cells, of the length varying between 80 μm and 150 μm (shown by white arrows). For A, B, C, D, and E - 2000×.

Figure 7. Elongated cells and round cells in monocyte population at Day 6 of cultivation on films of different compositions (1-4) and culture plate plastic (CP): (Ec) – elongated cells; (Rc) – round cells.

Table 1 – Physicochemical properties of PHA specimens

PHA composition, mol.%	M_w, kDa	D	C_x, %	T_{melt}, °C	T_{degr}, °C	T_c, °C
P(3HB) 100.0	920	2.12	76	178.4	275.8	97
P(3HB-co-4HB) 89.6/10.4	580	3.52	42	165.2	268.4	74
P(3HB-co-3HV) 90.0/10.0	676	3.48	64	164.5	269.6	82
P(3HB-co-3HHx) 90.3/9.7	550	3.32	49	162.4	270.0	72

Table 2 – Surface properties of the films prepared from PHAs with different chemical compositions

PHA composition, mol.%	Water contact angle, θ, degrees	Surface tension γ, erg/cm^2	Ra – arithmetic mean surface roughness, nm	Rq – root mean square roughness, nm
P(3HB) 100.0	70.0±0.4	32.8	71.7	80.2
P(3HB-co-4HB) 89.6/10.4	57.4±0.6	43.1	177.5	248.1
P(3HB-co-3HV) 90.0/10.0	60.3±2.8	40.7	172.3	206

P(3HB-co-3HHx) 90.3/9.7	60.9±1.6	42.4	158.2	198.5

Table 3 – Assessment of biological quality of erythrocytes after contacting with polymer films made from PHAs with different chemical compositions

PHA composition, mol.%	Starting proportions of the types of erythrocytes in the erythrocyte mass	Types of erythrocytes after contacting PHA films for 1 h at 22°C		
		Normal cells	Altered/ damaged cells	Dead cells
P(3HB) 100.0	Normal cells=85.2 Altered/ damaged cells=11.2 Dead cells=3.1	84.0	11.4	3.0
P(3HB-co-4HB) 89.6/10.4		86.1	10.2	2.4
P(3HB-co-3HV) 90.0/10.0		85.0	12.1	2.9
P(3HB-co-3HHx) 90.3/9.7		86.2	10.5	2.0

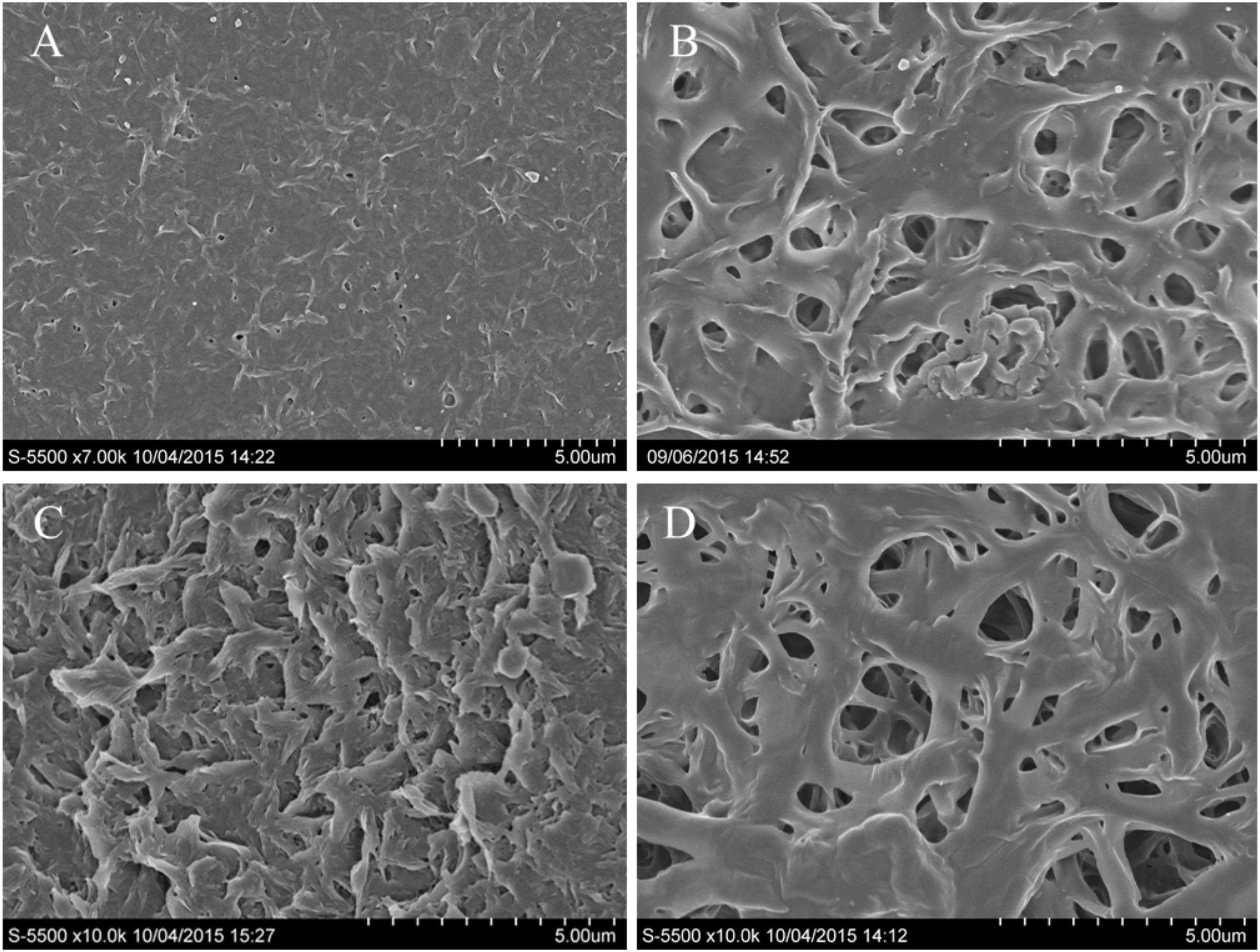
A
S-5500 x7.00k 10/04/2015 14:22
5.00um
B
09/06/2015 14:52
5.00um
C
S-5500 x10.0k 10/04/2015 15:27
5.00um
D
S-5500 x10.0k 10/04/2015 14:12
5.00um

Figure 1

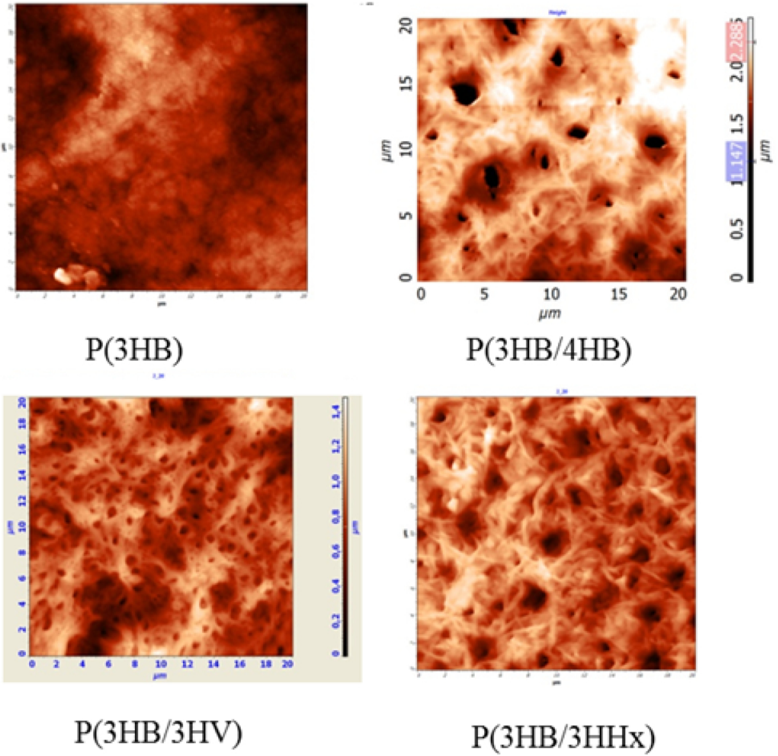

P(3HB)
P(3HB/4HB)
0
5
10
15
20
μm
2.0
1.5
0.5
2.288
1.147
P(3HB/3HV)
0
2
4
6
8
10
12
14
16
18
20
μm
0.2
0.4
0.6
0.8
1.0
1.2
1.4
P(3HB/3HHx)

Figure 2

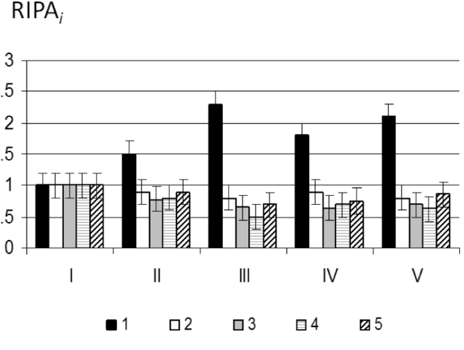

Figure 3

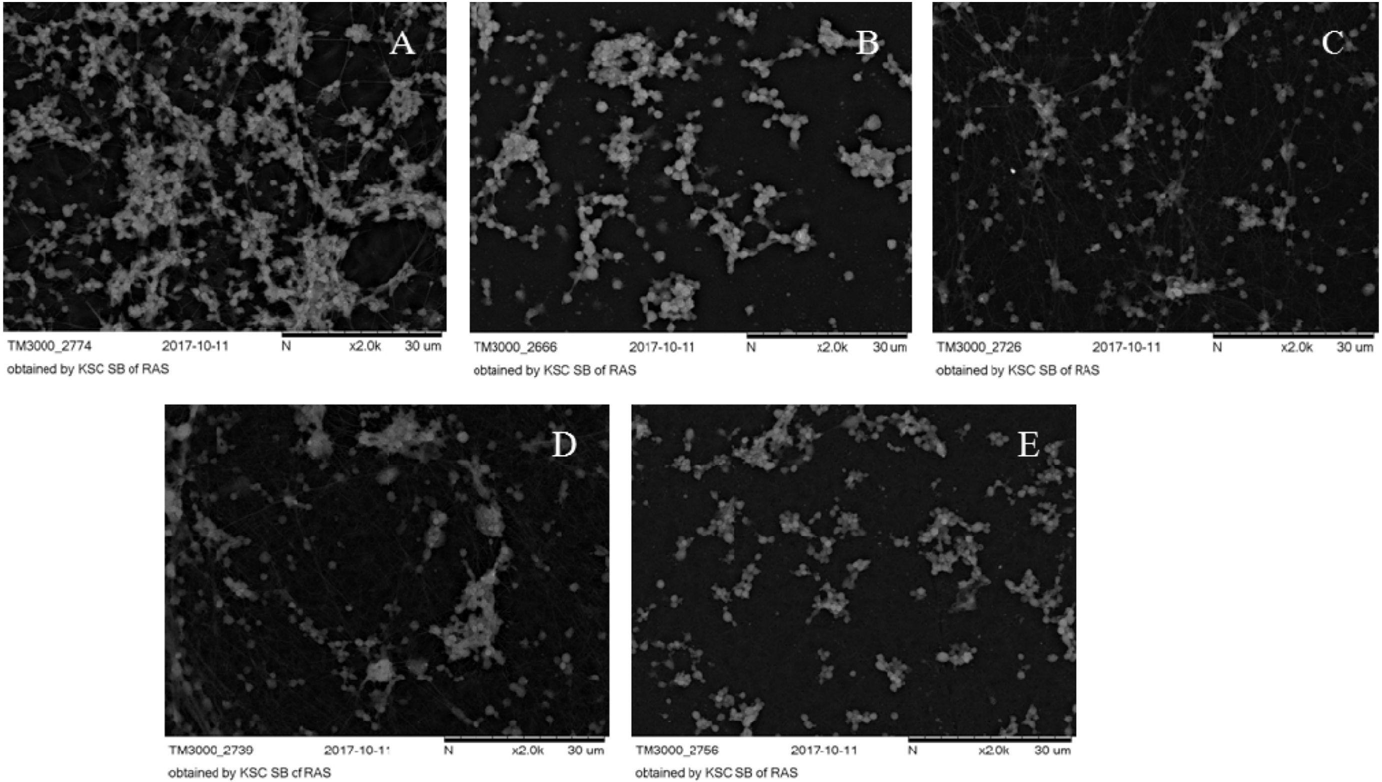
A
TM3000_2774 2017-10-11 N x2.0k 30 um
obtained by KSC SB of RAS
B
TM3000_2666 2017-10-11 N x2.0k 30 um
obtained by KSC SB of RAS
C
TM3000_2726 2017-10-11 N x2.0k 30 um
obtained by KSC SB of RAS
D
TM3000_2739 N x2.0k 30 um
obtained by KSC SB of RAS
E
TM3000_2756 2017-10-11 N x2.0k 30 um
obtained by KSC SB of RAS

Figure 4

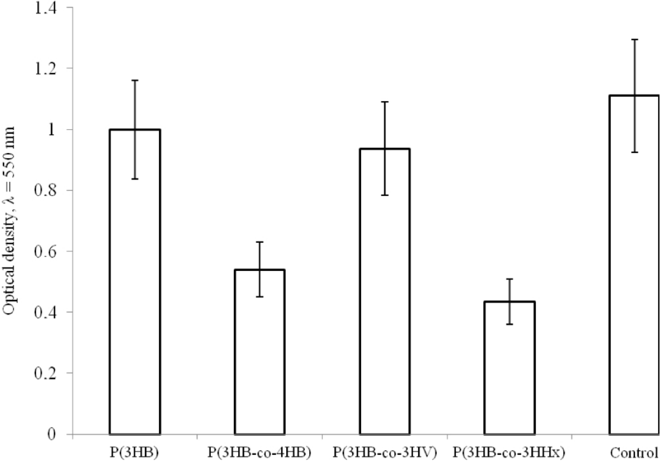

1.4
1.2
1
0.8
0.6
0.4
0.2
0
Optical density, λ = 550 nm
P(3HB)
P(3HB-co-4HB)
P(3HB-co-3HV)
P(3HB-co-3HHx)
Control

Figure 5

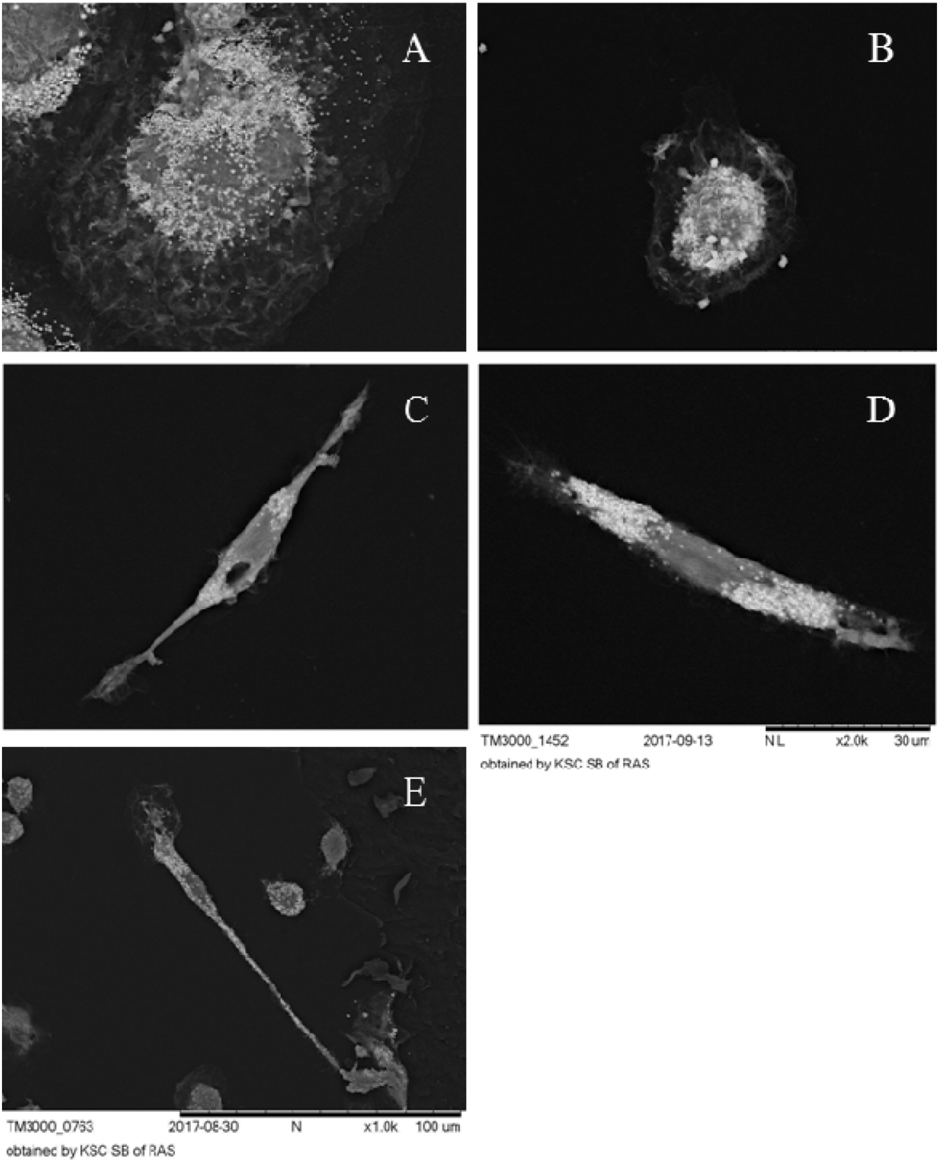
A
B
C
D
TM3000_1452
2017-09-13
NL
x2.0k
30 um
obtained by KSC SB of RAS
E
TM3000_0763
2017-08-30
N
x1.0k
100 um
obtained by KSC SB of RAS

Figure 6

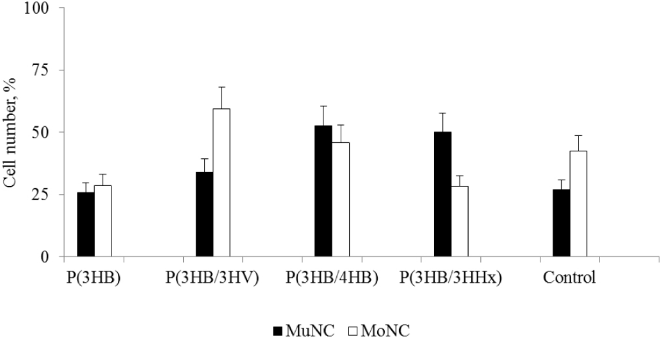
100
75
50
25
0
Cell number, %
P(3HB)
P(3HB/3HV)
P(3HB/4HB)
P(3HB/3HHx)
Control
MuNC
MoNC

Figure 7